Numerical study of particle-size distributions retrieved from angular light-scattering data using an evolution strategy with the Fraunhofer approximation

Javier Vargas-Ubera,[1,*] Juan Jaime Sánchez-Escobar,[2] J. Félix Aguilar,[1] and David Michel Gale[1]

[1]Instituto Nacional de Astrofísica Óptica y Electrónica (INAOE), Luis E. Erro No. 1, Tonantzintla Puebla, 72840 México
[2]Centro de Enseñanza Técnica Industrial (CETI), Nueva Escocia 1885, Frac. Providencia, Guadalajara Jalisco, 44620 México

*Corresponding author: thesis_234@yahoo.es

Received 20 November 2006; accepted 15 January 2007;
posted 2 February 2007 (Doc. ID 77188); published 18 May 2007

An algorithm is presented based on an evolution strategy to retrieve a particle size distribution from angular light-scattering data. The analyzed intensity patterns are generated using the Mie theory, and the algorithm retrieves a series of known normal, gamma, and lognormal distributions by using the Fraunhofer approximation. The distributions scan the interval of modal size parameters $100 \leq \bar{\alpha} \leq 150$. The numerical results show that the evolution strategy can be successfully applied to solve this kind of inverse problem, obtaining a more accurate solution than, for example, the Chin–Shifrin inversion method, and avoiding the use of *a priori* information concerning the domain of the distribution, commonly necessary for reconstructing the particle size distribution when this analytical inversion method is used. © 2007 Optical Society of America

OCIS codes: 290.0290, 290.3200, 290.4020, 290.5850.

1. Introduction

The estimation of particle size is an important task in a large range of industrial processes and technological applications. A frequently used optical technique is the analysis of the scattering pattern produced by the sample in the propagation direction. The estimation of a particle-size distribution (PSD) is an inverse problem rigorously treated by means of the Mie theory [1]. However, when the size of the scatterer becomes considerably larger than the wavelength of the light, and the relative refractive index between the scatterer and the medium differs substantially from unity, the dominant contribution to the near forward-scattered light can be described by the Fraunhofer approximation of the scalar diffraction theory [1].

The Fraunhofer approximation represents an asymptotic limit of the Mie theory, independent of the optical properties of the particles and the medium and is numerically easy to manage. The problem is solved either by a direct integral transform inversion method, known as the Chin–Shifrin method (CS) [2–8] or indirectly by using a numerical quadrature of the governing integral equation [8–10]. However, this asymptotic limit to the rigorous theory depends on initial information that must be provided by the user. The most significant disadvantage in these inversion schemes, is that we must suppose *a priori* the domain of the sought distribution. On the other hand, the evolutive algorithm obtains the PSD ignoring information about the domain, since it works as a nontraditional optimization method [11,12], which is based on the mechanisms of biological evolution.

An evolution strategy (ES) works with a set of potential solutions to the problem of interest, where each potential solution, called an individual, is represented by a vector of real numbers. This is a good representation when the problem at hand deals with continuous parameters. The main objective is to find a PSD starting from an intensity pattern, reduced to obtain a vector of real numbers that encodes an adequate solution, evaluated according to a fitness function that depends on the problem to be solved. The ES

0003-6935/07/173602-09$15.00/0

begins searching for a solution within a population of individuals, each of which represents not only a search point in the space of potential solutions to the given problem, but also may be a temporal container of current knowledge about the laws of the environment [13]. The starting population evolves toward successively better regions of the search space by means of processes of recombination, mutation, and selection. The recombination mechanism allows for mixing of parental information, which is passed on to their descendants, while mutation introduces innovation into the population [14]. The environment delivers a quality metric (fitness value) for each search point, and the selection process favors those individuals with higher quality to reproduce more often than weak individuals [13].

Thus our method retrieves a PSD from simulated angular light-scattering data by solving an optimization problem in the real domain, where an objective function [13] is minimized and the solution to the total scattered intensity equation is considered as an inverse problem.

In spite of its limitations, the Fraunhofer approximation continues to be used in problems where the optic properties of the particles and the medium that contains them are not so important, when the refractive index of the particles, the medium, or both are unknown, or simply when we do not have sufficient computation power for the numeric treatment of the problem. Numerical calculations using Mie theory are slow when the sample includes large particle sizes. In such cases, Mie theory requires the evaluation of series, which for convergence has a number of terms proportional [15] to the nondimensional size parameter $\alpha = ka$, with $k = 2\pi/\lambda$ the wavenumber, λ the wavelength of light in the medium, which surrounds the particles, and a the radius. This results in approximately 250 terms for $\lambda = 0.6328\ \mu\text{m}$ and $a = 25\ \mu\text{m}$, implying a factor of 4500 times more CPU time, compared with calculations performed using the Fraunhofer approximation. Although the ES increases the CPU time by a factor of 30 compared with the CS inversion method in the Fraunhofer approximation, this is still relatively small when compared with the CPU time used by the Mie theory.

In this work we consider three unimodal normal, gamma, and lognormal distributions centered at $\bar{\alpha} = 100$ and $\bar{\alpha} = 150$ over a fixed interval of sizes, and we use Mie theory to simulate an intensity pattern $I(\theta)$, where θ is the scattered angle. Then we retrieve the respective PSD by means of both the ES and the CS methods with the purpose of comparing the accuracy with which each method recovers the proposed distribution and the CPU time invested in each case.

In Section 2 we describe the formalism relating to the Fraunhofer approximation and the respective CS inversion method. Section 3 presents a generalized description of the algorithm implemented in this work. In Section 4 the main numerical results are presented. Finally conclusions are presented in Section 5.

2. Fraunhofer Approximation and the Chin–Shifrin Method

In the context of Mie theory the total scattered intensity $I(\theta)$, due to a proposed distribution $f(\alpha)$, is given by the following integral equation [1]:

$$I(\theta) = \int_0^\infty I(\theta,\ \alpha,\ m) f(\alpha) \mathrm{d}\alpha. \tag{1}$$

This is a Fredholm integral of the first kind in which the kernel $I(\theta, \alpha, m)$ represents the Mie-scattered intensity corresponding to a single particle of size parameter α and relative refractive index m in the annular region defined by the forward-scattering angle θ in the direction of propagation. $f(\alpha)$ is the particle density, such that $f(\alpha)\mathrm{d}\alpha$, is the number of particles with sizes between α and $\alpha + \mathrm{d}\alpha$.

When the Fraunhofer approximation is used, the kernel does not depend on the relative refractive index since $I(\theta, \alpha)$ is modeled as the Airy pattern produced by an opaque disk of radius a equivalent to that of the particle of size parameter α. Hence from Eq. (1) the total intensity is given by [1]

$$I(\theta) = \frac{I_0}{k^2 F^2} \int_0^\infty \frac{\alpha^2 J_1{}^2(\alpha\theta)}{\theta^2} f(\alpha) \mathrm{d}\alpha, \tag{2}$$

where I_0 is the incident beam intensity, J_1, is the Bessel function of the first kind and order one, and F is the focal length of the receiver lens, as typically encountered in laser diffraction particle size analyzers. In this paper the integrals in Eqs. (1) and (2) are calculated numerically using the trapezoidal rule in the finite interval in which the proposed distribution is defined. These intensity patterns were generated for a common angular region $0.0573° \leq \theta \leq 10.886°$, with angular sampling $\Delta\theta = 0.0458°$ and 40 subdivisions in size $\Delta\alpha$.

Equation (2) accepts an asymptotic analytic solution, widely referred to in the literature as the CS method [4,7]:

$$f(\alpha) = \frac{-2\pi k^3 F^2}{\alpha^2} \int_0^\infty (\alpha\theta) J_1(\alpha\theta) Y_1(\alpha\theta) \frac{\mathrm{d}}{\mathrm{d}\theta}\left[\theta^3 \frac{I(\theta)}{I_0}\right] \mathrm{d}\theta, \tag{3}$$

where, Y_1 is the Bessel function of the second kind and order one.

This solution is a direct integral transform inversion method in that the integrand directly contains the measured intensity. Once again the integral in Eq. (3) is calculated numerically by means of the trapezoidal rule, and the derivative is calculated by the finite differences method.

In the numerical evaluation of Eqs. (2) and (3), it is important to recognize the differences in both the size and angular domains because *a priori* we suppose

that the major contribution to the integral occurs only for a finite interval in sizes and for θ in the range from θ_{min} to θ_{max} limited by the validity of the paraxial approximation. The truncation by θ_{max} leads to a decrease of the performance in the retrieval function using this method.

3. Proposed Algorithm

This recuperation method is based on the evolutive algorithm described by Vázquez-Montiel *et al.* [14]. To produce offspring we used the recombination and mutation operators such as those described in the previous work. The selection operator was performed using the configuration $(\mu + \beta)$ [13]. In this notation μ represents the set of parents and β the set of offspring, so the best individuals are chosen for the next iteration from the set of parents and offspring; thus the proposed algorithm produces an enlarged sampling because both parents and offspring have the same chance of competing for survival. As a result a deterministic search is performed to find the solution within the space of potential solutions.

To perform the proposed algorithm each individual $\vec{x}_\ell$ is formed by the vector of elements called object variables $x_{\ell,p}$ with a respective strategy parameter $\xi_{\ell,p}$ [14].

$$\vec{x}_\ell = [x_{\ell,p},\ \xi_{\ell,p}], \quad \text{where}, p = 1, \ldots, 5. \tag{4}$$

Thus each individual represents the set of parameters necessary to describe a PSD, given by means of the following assignation:

$$x_{\ell,1} \equiv \text{mean size parameter},$$

$$x_{\ell,2} \equiv \text{standard deviation},$$

$$x_{\ell,3} \equiv \text{first size parameter},$$

$$x_{\ell,4} \equiv \text{second size parameter},$$

$$x_{\ell,5} \equiv \text{smallest size parameter}, \tag{5}$$

where "first size parameter" and "second size parameter" correspond to the finite interval in which the distribution is defined.

The genetic operators of recombination and mutation work with all the extended vector $\vec{x}_\ell$ from Eq. (4), because it contains the standard deviation for carrying out the mutation.

The process of evaluating the fitness of an individual $\vec{x}_\ell$ consists of the following two steps [14]:

- An intensity pattern I_ℓ is constructed from $\vec{x}_\ell$ by substituting only the first five elements of $\vec{x}_\ell$ from Eq. (4) to generate the distribution $f(\alpha)$. Equation (2), is then used to calculate the total scattered intensity.
- Considering each element in the matrix I_ℓ as a dimension in a Euclidian distance space, we assign as the fitness the Euclidian distance between I_ℓ and the reference intensity pattern represented by I_{ref}. Thus the fitness is given by

$$\text{fitness} = \sqrt{\sum_{i=1}^{j} [I_{\ell_i} - I_{ref_i}]^2}, \tag{6}$$

where j is the number of elements in the intensity pattern.

We have chosen this fitness function because it evaluates the minimum distance between the optimized intensity and the simulated intensity for a specific number of iterations. This function represents a measure of the quality of the solution that the best individual of a population contains in its structure. In our numerical results, this particular fitness function and the operators of recombination, mutation, and selection accomplish a mapping with a high correlation between the objective function and the proximity to the zone where the correct solution or optimal solution resides.

Rechenberg [11] proposed a deterministic adjustment of strategy parameters during evolution called the "1/5 − success rule," which reflects that, on average, one output from every five mutations should cause an improvement in the objective function values to achieve best convergence rates. If more than 1/5 of the mutations are successful, the strategy parameter ξ is increased, otherwise it is decreased. The selection operator evaluates Eq. (6) for the total population and chooses the best M individuals that will in turn form the new generation of solutions.

Our program was implemented in MATLAB programming language since it allows an algorithm to be written in the simplest form. We note that MATLAB is called an interpreter because it first interprets the operations, and then the operations are performed. As a result we have a slow algorithm. However, a compiler such as Fortran provides a series of optimizations that can help speed up the compiled code. An analysis of this option is not intended to form part of this paper.

4. Numerical Results

Each numerical realization took approximately 30 min to run on a PC with a Pentium IV processor under the following conditions: A population equal to $M = 50$ is used throughout; the recombination operator is applied to the set of parents to obtain 30% of offspring, while the mutation operator provides the remaining 70%. Thus the set of parents and offspring has a similar number of individuals. The aptitude related to each individual was determined by using Eq. (6). The selection operator chooses the best M individuals from the set of $2M$ parents and offspring for the next iteration $t = t + 1$ by means of a ranking procedure. In each iteration we use the output of the best individual to plot the behavior of the objective function. This cycle is repeated until we obtain a goal value such that the objective function is minimized, or when a fixed number of iterations is reached. This stop criterion was fixed after testing different distri-

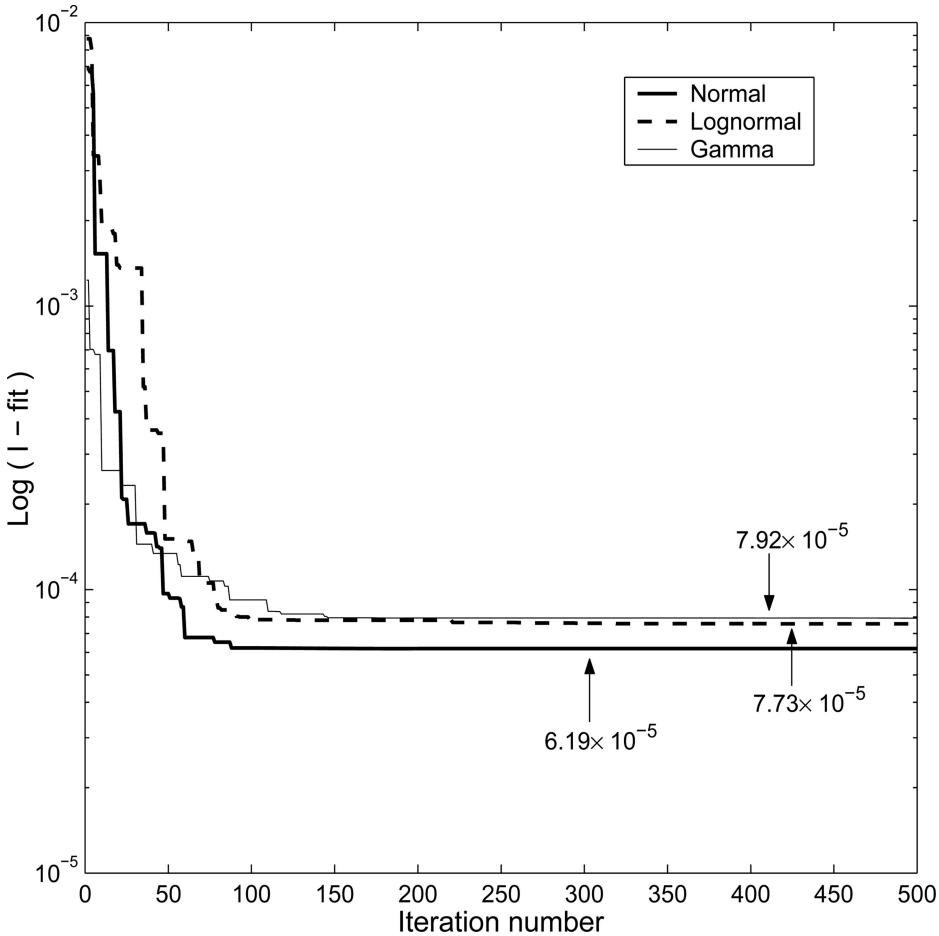

Fig. 1. Typical behavior in the minimization of the objective function for normal, gamma, and lognormal retrieved distributions in the medium size range.

butions. In Fig. 1 we illustrate the typical behavior of the objective function for the three kinds of distribution analyzed in this study.

The objective function never reaches the proposed goal value of 10^{-9}; hence we fixed the maximum number of iterations at 500 as a threshold value and the goal value 10^{-9} as our stop criterion in the algorithm. We observe good convergence of the three distributions for 100 iterations. When the stop criterion is reached, our result is the best individual of the last generation, represented by a vector, which corresponds to the PSD that best matches the analyzed intensity pattern.

Figure 2 contains several plots that compare the logarithm of the optimized intensity pattern produced by the ES with the theoretical intensity patterns calculated using Mie theory, normalized with total incident intensity. Figures 2(a)–2(c) correspond to the normal, lognormal, and gamma distributions, respectively, as used in Fig. 1. We can see that the optimized intensity patterns, shown by the dotted curves of Fig. 2, are in agreement with the values of the objective function. The optimized pattern shows evident discrepancies. This behavior suggests that fit errors of the order of 10^{-5} or smaller will generate a high degree of similarity between intensity patterns, as shown in Fig. 2. Nevertheless, in this work we considered 10^{-9} as a goal value to assure the best results.

A. Evolution Strategy and the Chin–Shifrin Method in the Recuperation of a Normal Distribution

The aim of this first part of our numerical study is to analyze the behavior of the ES with respect to the CS inversion method when the intensity pattern is calculated by means of rigorous Mie theory, and the recuperation is realized with the Fraunhofer approximation. We choose two characteristic size ranges where the use of the Fraunhofer approximation is feasible. For this work we have analyzed three different kinds of distribution; however, for the present discussion it is enough to consider only the results obtained for normal distributions since they illustrate adequately the advantages of our algorithm in comparison with the results given by the CS method.

The two normal distributions analyzed cover the range $30 \leq \alpha \leq 200$, centered at $\bar{\alpha} = 100$, and $50 \leq \alpha \leq 250$ centered at $\bar{\alpha} = 150$. We will refer to them as medium and large sizes, respectively. It has been shown by several authors that the Fraunhofer approximation describes well the scattering phenomena produced by spherical particles in this range of size

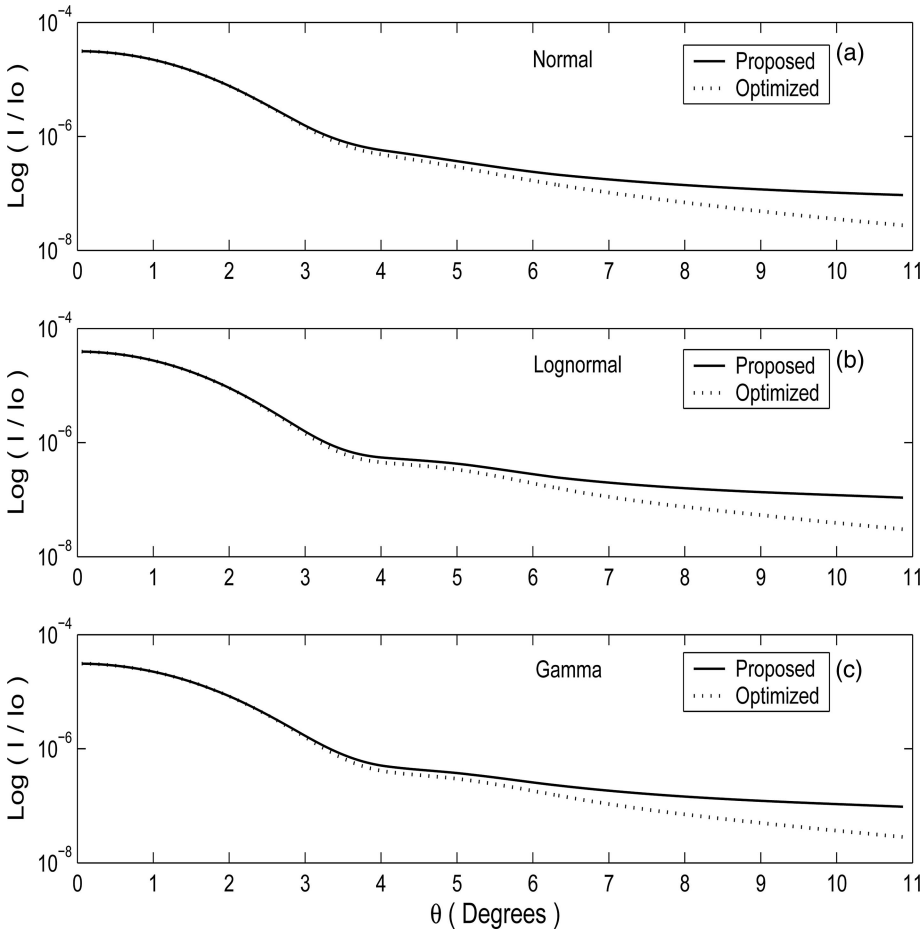

Fig. 2. Comparison between the retrieved scattering pattern produced by the ES and the simulated intensity patterns calculated with Mie theory. The plots correspond to the three distributions presented in Fig. 1: (a) normal, (b) lognormal, and (c) gamma.

parameters [2,6,16]. The intensity patterns were generated with the same mesh and common angular region used in the evaluation of the numerical integrals calculated in Section 2. The parameters that control the shape of the two normal distributions discussed here are presented in Table 1.

For the two distributions mentioned above, we generate an intensity pattern by means of Mie theory, then using the Fraunhofer approximation together with our algorithm we obtain a first retrieved PSD, and with the Fraunhofer approximation and the CS method we obtain a second retrieved PSD as shown in Fig. 3. This figure illustrates adequately both the good behavior of the ES in the recuperation and the poor results reported by the CS inversion method.

Table 1. Shape Parameters of the Proposed Distribution Functions[a]

PSD Proposed	Normal		Gamma			Lognormal		
Size ranges	$\bar{\alpha}$	σ	ϵ	υ	α_0	A_0	σ	α_0
Medium	100	20	90	0.6	29.9	76	2.7	29.9
Large	150	30	125	0.7	49.9	107	2.9	49.9

[a]A particle number $N = 100$ is used throughout. $\bar{\alpha}$ and σ represent the mean size parameter and the standard deviation in normal distributions, respectively. ϵ and υ are the effective size parameter and the variance in gamma distributions. In the lognormal distributions, σ is the standard deviation, and A_0 is a quantity related with the mean size parameter of an equivalent normal distribution through $\bar{\alpha} = \exp[\ln(A_0) + (\sigma^2/2)]$. α_0 determines the smallest size parameter present in the gamma and lognormal distributions.

The differences between the retrieved and proposed distributions can be considered as an indicator of error in the recuperation, which is estimated by means of the standard deviation

$$s = \frac{1}{N_s}\sqrt{\sum_{i=1}^{N_s}\frac{(f_{ref_i} - f_{\ell_i})^2}{{f_{ref_i}}^2}}, \tag{7}$$

where f_{ref_i} and f_{ℓ_i} are the i values of the proposed and the retrieved distributions, respectively, and N_s is the number of points calculated. Both error values, those relating to the CS method and those associated with our algorithm are shown for the corresponding curves by arrows in Fig. 3. Figure 3(a) represents the medium size range, and Fig. 3(b) represents the large size range. Corresponding fit errors between the simulated intensity patterns and the intensity patterns reported at the end of the optimization process in the ES were 6.1934×10^{-5} and 1.4415×10^{-5} for the medium and large sizes, respectively. These results will be discussed further in Subsection 4.B.

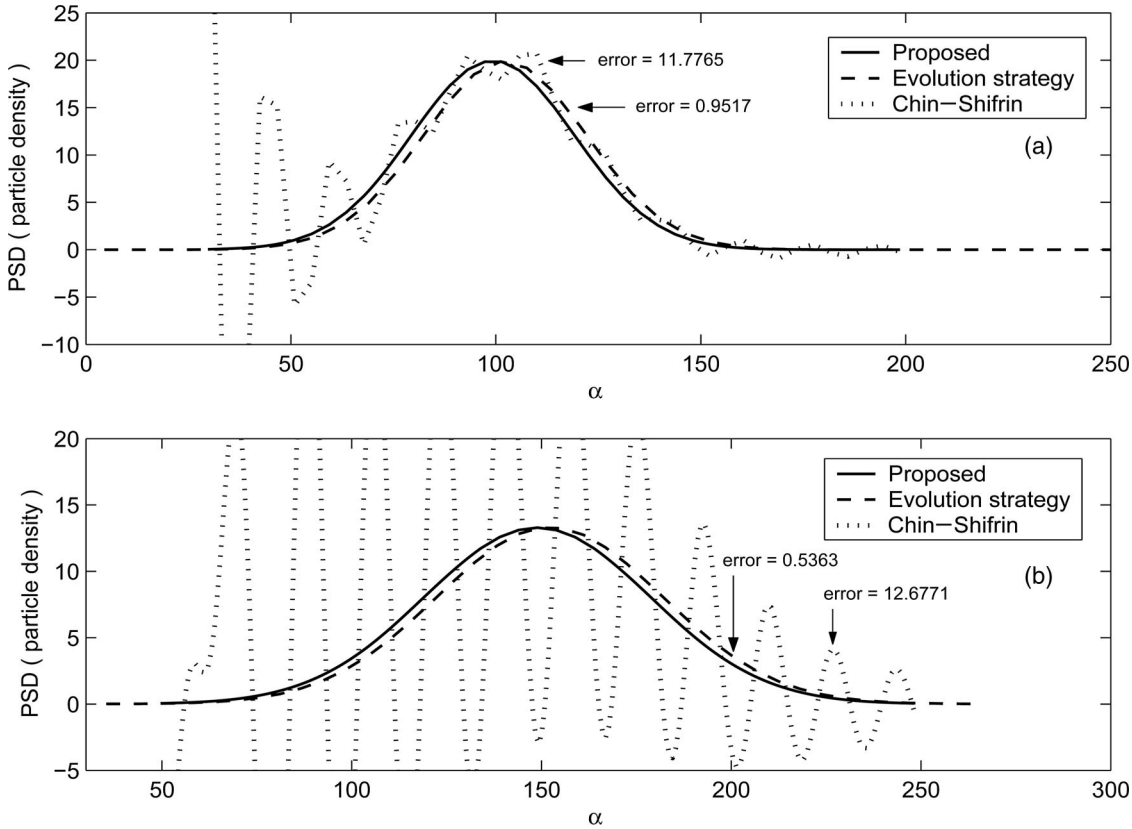

Fig. 3. Comparison between the ES and the CS methods applied to the recuperation of a normal distribution. (a) Medium size region and (b) large size regions.

Figures 3(a) and 3(b) show that for both regions chosen for α, the ES generates superior results. We note also from Fig. 1 that the fit error between the calculated and ES intensity patterns remains almost constant from iteration number 100. This confirms that our algorithm finds the closest solution to the global optimum. Remember again that the ES method is capable of obtaining the correct results without any *a priori* information regarding the distribution interval, and that the possible discrepancies in the angular composition of the scattered intensity do not affect the performance of the algorithm, as happens in general when the Fraunhofer approximation is applied to solve the inverse problem by quadratures, and again with the CS method. This last point is clearly observed with the CS recuperation in Fig. 3. We can conclude that in the particular case of medium and large particles, the Fraunhofer approximation implemented using an ES algorithm obtains accurate results.

Finally the Fig. 3 results show the poor quality of the recuperation using the CS method. Thus, it is not recomended to use this inversion method with the Fraunhofer approximation for these size ranges.

B. Robustness of the Evolution Strategy for Retrieval of a Particle Size Distribution

In this second part of our numerical study, we show the robustness of the ES implemented in our algorithm with the Fraunhofer approximation. Given the intensity pattern corresponding to a known distribution, our algorithm selects among the three kinds of distribution under consideration, finding that which can be satisfactorily fitted to this original intensity pattern. This procedure is carried out adjusting the simulated intensity pattern, with the intensity pattern generated by each kind of distribution sequentially inside the algorithm evaluating the fit error between both patterns. The corresponding retrieved distributions are then compared with the proposed theoretical distribution, and the recuperation error between both distributions is obtained. The smallest values of both errors determines the best retrieved distribution that the algorithm can obtain. The best result (smaller errors) coincides with the proposed distributions.

To generate the simulated intensity pattern, we consider only the gamma and lognormal distributions, since the performance of the ES method with normal distributions was discussed in Subsection 4.A and produces similar results. Again we consider two intervals, similar with respect to the previous numerical simulations, representing medium and large particle size ranges, and we employ the same domain and angular sampling parameters that we used in the previous section.

Figure 4 shows the behavior of our algorithm for both distributions. As can be seen, the performance of

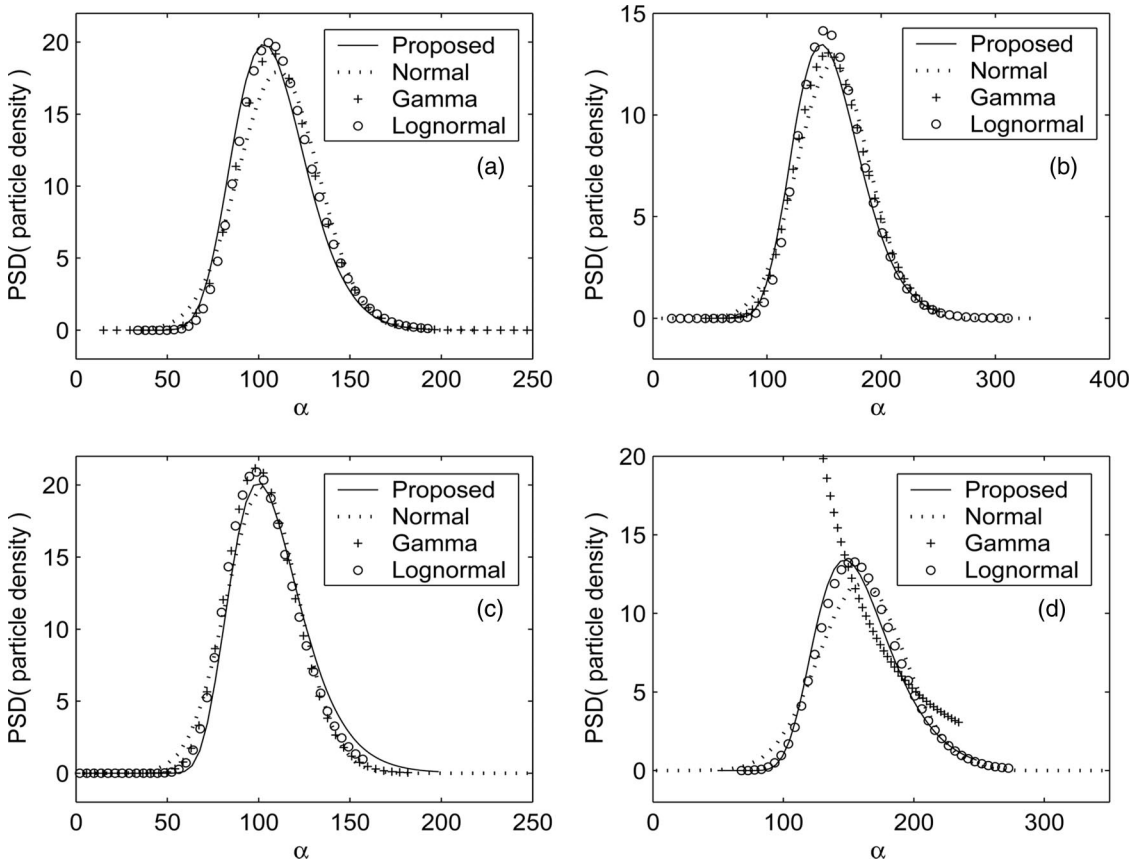

Fig. 4. Recuperation with the ES from the intensity pattern generated by gamma and lognormal distributions in medium and large size ranges. (a) and (b) correspond to normal, gamma, and lognormal distributions retrieved by the ES from the intensity pattern generated by Mie theory with a gamma distribution at the medium and large sizes. (c) and (d) correspond to normal, gamma, and lognormal distributions retrieved by the ES from the intensity pattern generated by Mie theory with a lognormal distribution at the medium and large sizes.

the ES is similar with respect to the previous numerical simulations. Figures 4(a) and 4(b) correspond to the intensity patterns generated by gamma distributions in both size ranges, while Figs. 4(c) and 4(d) correspond to the intensity patterns generated by the lognormal distributions.

The curves display an identical numerically retrieved PSD, and we can see in Table 2 that the fit error and the recuperation error are a minimum (in boldface) when the ES algorithm selects the gamma distribution. In Figs. 4(a) and 4(b) both normal distributions (dotted curves) and lognormal distributions (circled curves) are retrieved from the intensity pattern generated by the above-mentioned gamma distribution. In the first case, the fit error and the recuperation error increase because when the ES transforms the fitting problem into an optimization problem the solution found is not near-optimal. On the other hand, when the proposed distributions are analyzed with lognormal distributions our algorithm gives a better result. Here the recuperated lognormal distributions are closer to the proposed distribution in the medium and large range; however, as mentioned above, the minimal recuperation error is obtained when our algorithm analyzes the proposed distribution with the gamma distribution. We conclude that the ES is able to recognize the correct distribution among the three possibilities of distributions mentioned above.

Table 2. Errors for Proposed Gamma Distributions[a]

PSD	Gamma-Medium		Gamma-Large	
Error	I-fit	PSD	I-fit	PSD
N	9.97×10^{-5}	1.84	2.05×10^{-4}	1.14
G	7.92×10^{-5}	**1.02**	1.73×10^{-4}	**0.67**
L–N	8.28×10^{-5}	1.14	1.91×10^{-4}	0.72

[a]Column I-fit represents the fit errors between the simulated intensity pattern with a gamma distribution and the intensity pattern reported by the ES to each kind of distribution. Column PSD represents the errors of recuperation between the proposed and the retrieved distributions.

We now look at the two lognormal distributions shown in Figs. 4(c) and 4(d). The dotted curves show a numerically resolved size-distribution recovery identical to the normal distributions in both regions as before. Recovery with the gamma distribution is acceptable in the medium region; however, for the region of large particles, the retrieved distribution in Fig. 4(d) is very poor. Table 3 shows the fitting and

Table 3. Errors for Proposed Lognormal Distributions[a]

PSD	Lognormal-Medium		Lognormal-Large	
Error	I-fit	PSD	I-fit	PSD
N	1.21×10^{-4}	1.18	2.15×10^{-4}	1.35
G	1.46×10^{-4}	1.24	1.85×10^{-4}	9.59
L–N	7.73×10^{-5}	**1.12**	1.71×10^{-4}	**0.66**

[a]Column I-fit represents the fit errors between the simulated intensity pattern with a lognormal distribution and the intensity pattern reported by the ES to each kind of distribution. Column PSD represents the errors of recuperation between the proposed and the retrieved distributions.

recuperation errors corresponding to all curves of Figs. 4(c) and 4(d).

Regarding the fit with a lognormal distribution, we can see from Figs. 4(c) and 4(d) and Table 3 that this distribution (circles) generates superior results, with the recuperation practically identical to the proposed distribution. Again, in the particular case of a lognormal distribution used to generate an intensity pattern, the ES gives the best results, and it can be commented that the asymmetry of the distributions in both ranges of sizes of particles does not affect the performance of our algorithm.

From the above numerical simulations and for these three particular distributions we can conclude that the ES is independent of the type of monomodal distribution that we use. The ES can be adjusted with a distribution type unrelated to the proposed size distribution, though obviously with a lesser degree of accuracy in the results. However, this method can still be of value when information regarding the sought distribution is not available, or when the only important task is to give a diagnosis of the size of the particles and not the distribution type.

Finally, it is important to point out that our algorithm can analyze only distribution functions with up to a maximum of six optimization variables. If our method uses more than six optimization variables it cannot perform a search within the space of potential solutions. With a maximum of six variables our algorithm converges to an accurate solution at approximately the 100th generation in the simplest situations and at approximately the 420th generation when the problem is more numerically complex. During each experiment our method required more CPU time than the CS method, 30 min in our case, compared with 57 s for the CS method. When information about the sought distribution is unknown, it is preferable to consume more computing time.

5. Conclusions

In this work we have presented a method based on evolutionary computation to retrieve particle-size distributions from angular light-scattering data. Our method analyzes intensity patterns generated using Mie theory, giving as a result a series of known monomodal normal, gamma, and lognormal distributions by means of the Fraunhofer approximation. The proposed method introduces two important characteristics when compared to the traditional Chin–Shifrin method: We have obtained solid results that show that our program yields more accurate solutions compared to the Chin–Shifrin method and does not require *a priori* information about the domain of the particle-size distribution that we are seeking. The only requirement at the beginning of each optimization process is for information related to the simulated intensity pattern and a group of possible candidates of distributions in order to carry out the adjustment and obtain the corresponding particle-size distribution.

For the particular case of the three kinds of distribution discussed in this work, the performance of our program is not dependent on the type of monomodal distribution that we are analyzing. Accurate results are obtained for both symmetrical and asymmetrical distributions, and the method is able to identify the correct distribution from the three distribution types presented. The results are less accurate but still satisfactory when our method is applied to a distribution type unrelated to the proposed size distribution. This can be important when information on the original distribution is unavailable or when only a diagnosis of sizes present in the sample is required. We note that possible discrepancies in the angular composition of the scattered intensity do not affect the performance of the algorithm, unlike the case when the Fraunhofer approximation is used to solve the inverse problem by quadratures or with the CS method.

We propose a threshold value of 500 for the number of iterations and the goal value 10^{-9} as a general stop criterion when this algorithm is used. These values guarantee the correct convergence in the objective function, such that our algorithm can find the closest solution to the optimum global.

This inversion method based on evolutionary computation demonstrates high precision and acceptable computing time, providing the evolutive operators are used with a correct objective function. However, we have analyzed only distribution functions considering up to six optimization variables as a maximum. At present, this limitation does not allow us to retrieve more complex distributions, such as multimodal.

References

1. H. C. Van de Hulst, *Light Scattering by Small Particles,* 2nd ed. (Dover, 1981).
2. A. L. Fymat, "Analytical inversions in remote sensing of particle-size distributions. 2: Angular and spectral scattering in diffraction approximations," Appl. Opt. **17,** 1677–1678 (1978).
3. J. Liu, "Essential parameters in particle sizing by integral transform inversions," Appl. Opt. **36,** 5535–5545 (1997).
4. J. H. Koo and E. D. Hirleman, "Synthesis of integral transform solutions for the reconstruction of particle-size distributions from forward-scattered light," Appl. Opt. **31,** 2130–2140 (1992).
5. S. D. Coston and N. George, "Particle sizing by inversion of the optical transform pattern," Appl. Opt. **30,** 4785–4794 (1991).
6. J. C. Knight, D. Ball, and G. N. Robertson, "Analytical inversion for laser diffraction spectrometry giving improved resolution and accuracy in size distribution," Appl. Opt. **30,** 4795–4799 (1991).

7. J. B. Riley and Y. C. Agrawal, "Sampling and inversion of data in diffraction particle sizing," Appl. Opt. **30,** 4800–4817 (1991).
8. Z. Ma, H. G. Merkus, and B. Scarlett, "Particle-size analysis by laser diffraction with a complementary metal-oxide semiconductor pixel array," Appl. Opt. **39,** 4547–4555 (2000).
9. L. C. Chow and C. L. Tien, "Inversion techniques for determining the droplet size distribution in clouds: numerical examination," Appl. Opt. **15,** 378–383 (1976).
10. E. D. Hirleman, "Optimal scaling of the inverse Fraunhofer diffraction particle sizing problem: the linear system produced by quadrature," Part. Charact. **4,** 128–133 (1987).
11. I. Rechenberg, *Cybernetic Solution Path of an Experimental Problem* (Royal Aircraft Establishment, Library Translation No. 1122, August 1965).
12. H. J. Bremermann, "Optimization through evolution and recombination," in *Self-Organizing Systems,* M. C. Yovits, G. T. Jacobi, and G. D. Goldstine, eds. (Spartan Books, 1962), pp. 93–106.
13. T. Back, *Evolutionary Algorithms in Theory and Practice,* 1st ed. (Oxford U. Press, 1996).
14. S. Vázquez-Montiel, J. J. Sánchez-Escobar, and O. Fuentes, "Obtaining the phase of an interferogram by use of an evolution strategy: Part I," Appl. Opt. **41,** 3448–3452 (2002).
15. C. F. Bohren and D. R. Huffman, *Absorption and Scattering of Light by Small Particles,* 2nd ed. (Wiley, 1983).
16. J. Vargas-Ubera, J. F. Aguilar, and D. M. Gale, "Reconstruction of particle-size distributions from light-scattering patterns using three inversion methods," Appl. Opt. **46,** 124–132 (2007).